

Supporting Information

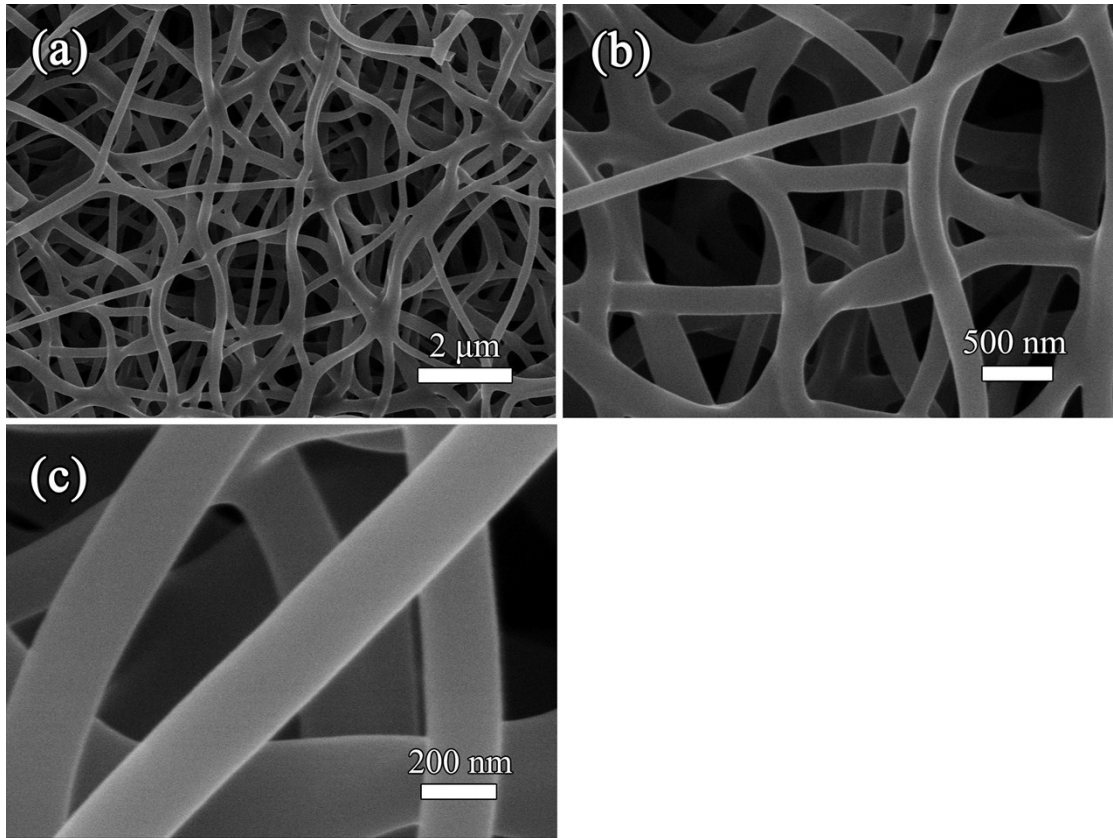


Fig. S1. (a-c) SEM image of N-doped carbon nanofibers (NCNFs)

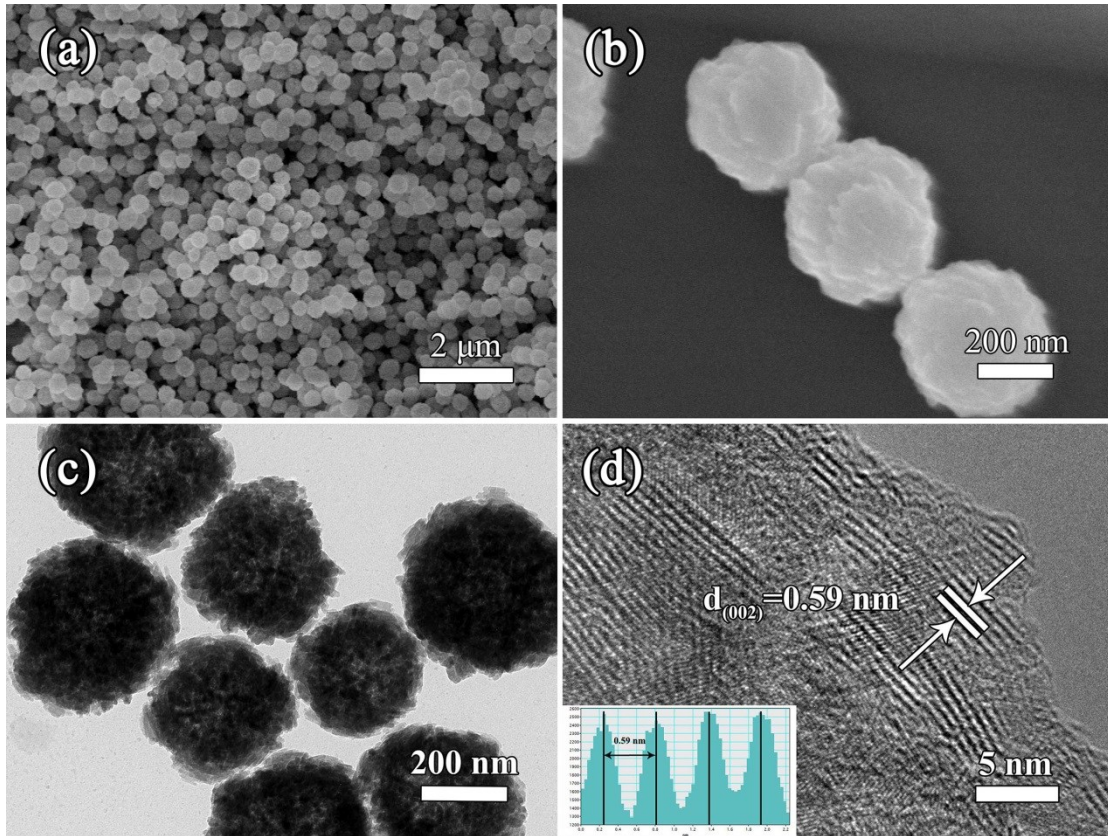


Fig. S2. (a, b) SEM images and (c,d) TEM images of VS₄ microspheres.

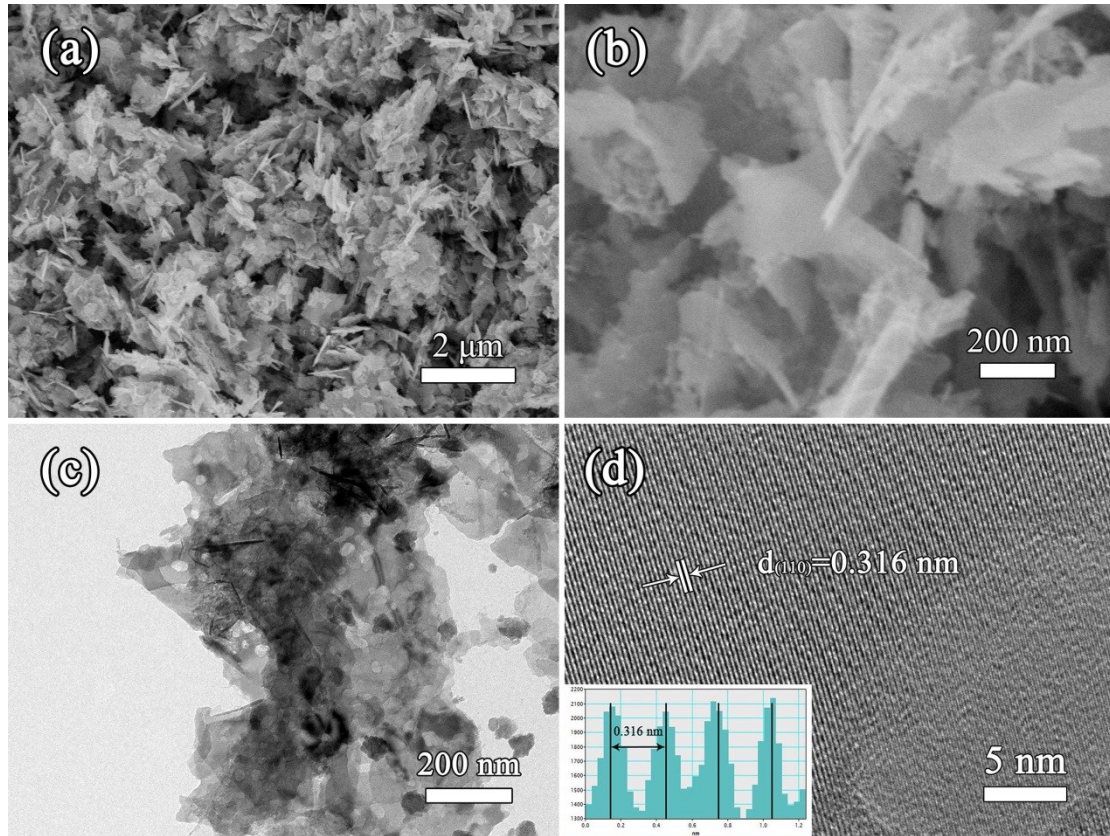


Fig. S3. (a, b) SEM images and (c,d) TEM images of bare V_3S_4 nanosheets.

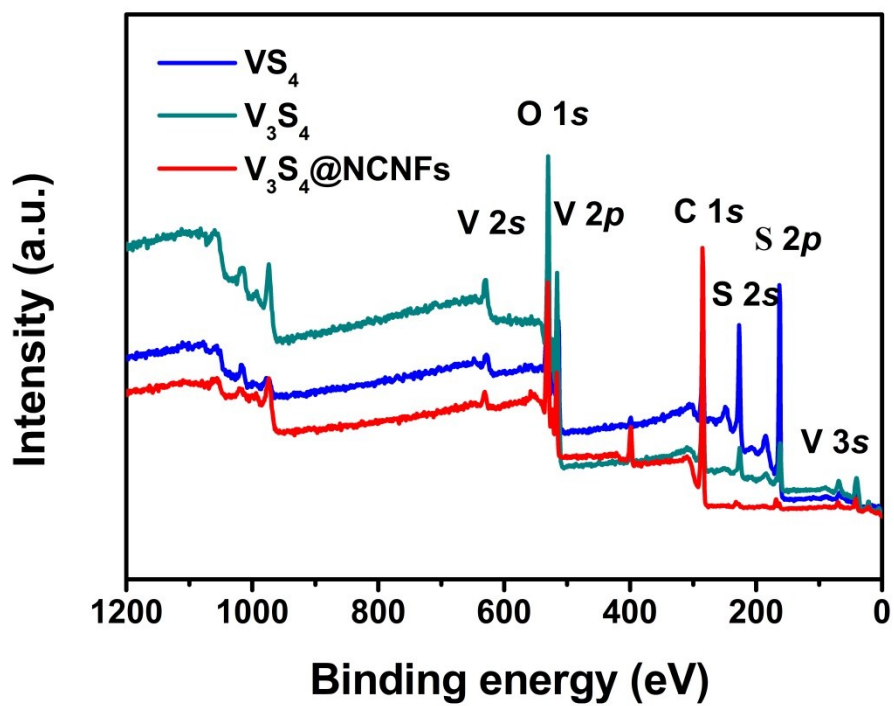


Fig. S4. XPS survey spectrum of VS_4 , bare V_3S_4 , and $V_3S_4@NCNFs$ composites.

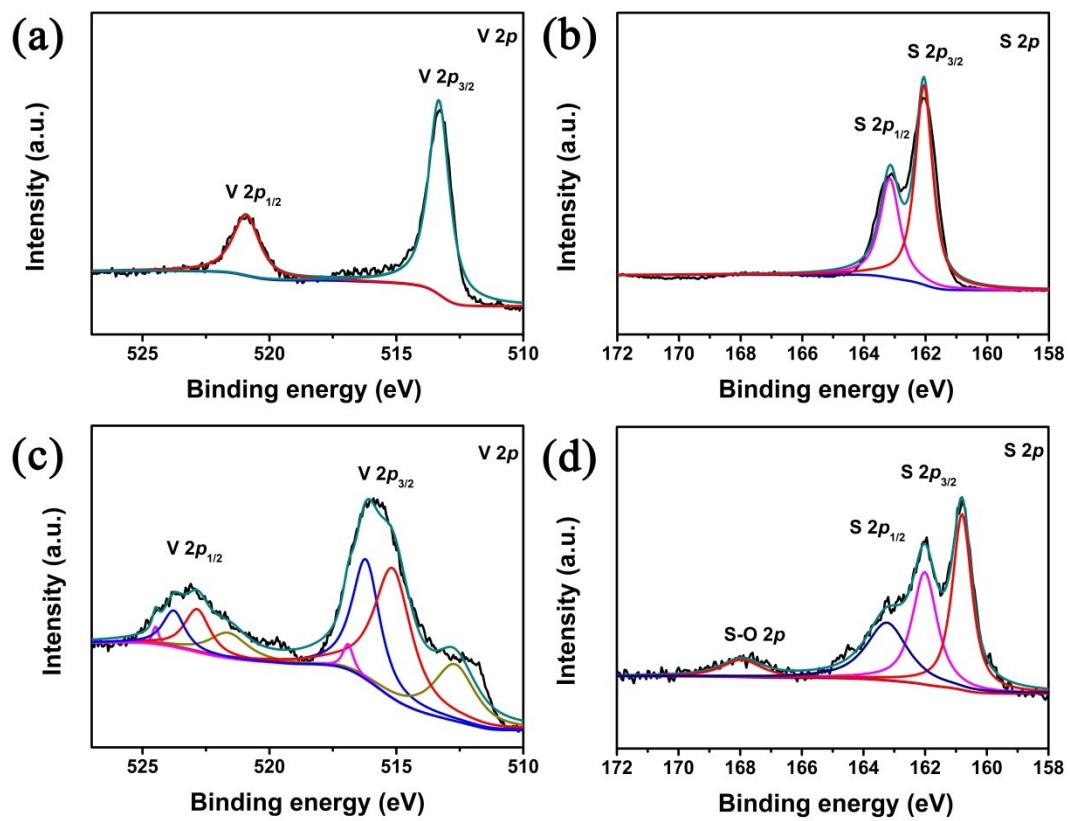


Fig. S5. The high-resolution XPS spectra of VS₄ (a, b), bare V₃S₄ (c, d) with V 2p, S 2p, respectively.

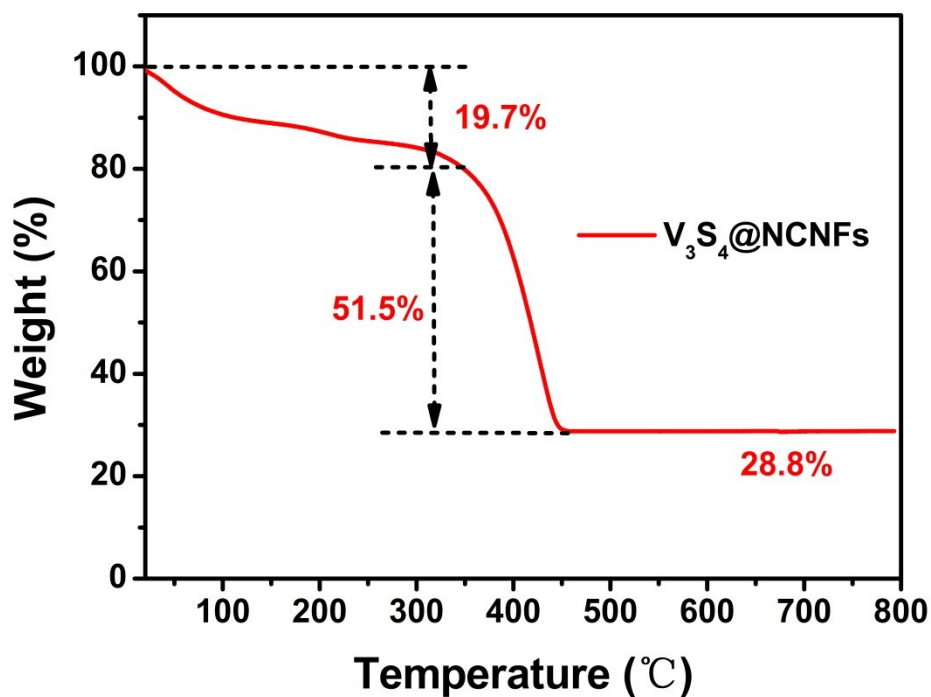
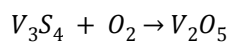


Fig. S6. TGA curves of V₃S₄@NCNFs sample in air from room temperature to 800 °C.

The initial mass loss below 350 °C is ascribed to the oxidation of V₃S₄ into V₂O₅ and the evaporation of water, and the distinct weight loss between 350 and 450 °C could be attributed to the carbon combustion with O₂ into CO₂. The mass ratios of V₃S₄ in these composites are calculated:



$$V_3S_4(\text{wt}\%) = 100 \times \frac{2 \times M V_3S_4}{2 \times M V_2O_5} \times \frac{m V_2O_5}{m V_3S_4@NCNFs}$$

$$= 29.7\%$$

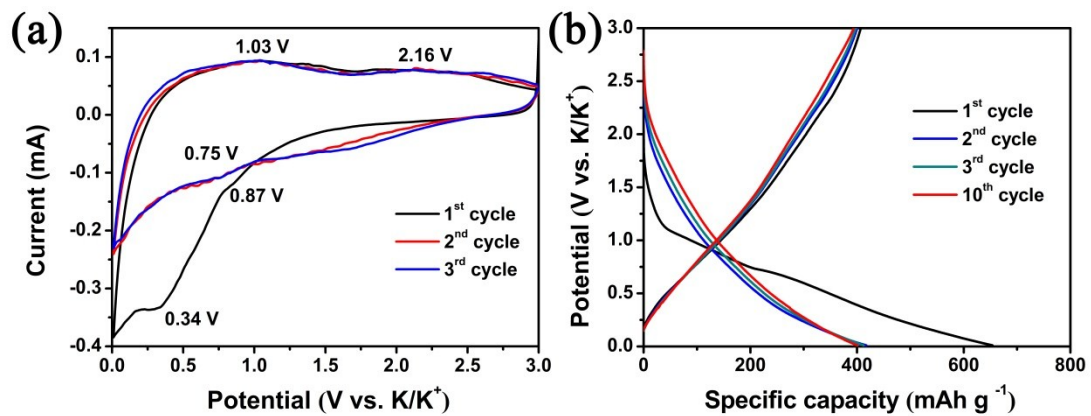


Fig. S7. (a) CV curves of $V_3S_4@NCNFs$ electrode at a scan rate of 0.2 mV s^{-1} in the potential of 0.01–3.0 V (vs. K/K^+). (b) Galvanostatic charge/discharge profiles of $V_3S_4@NCNFs$ at a current density of 0.2 A g^{-1} for PIBs.

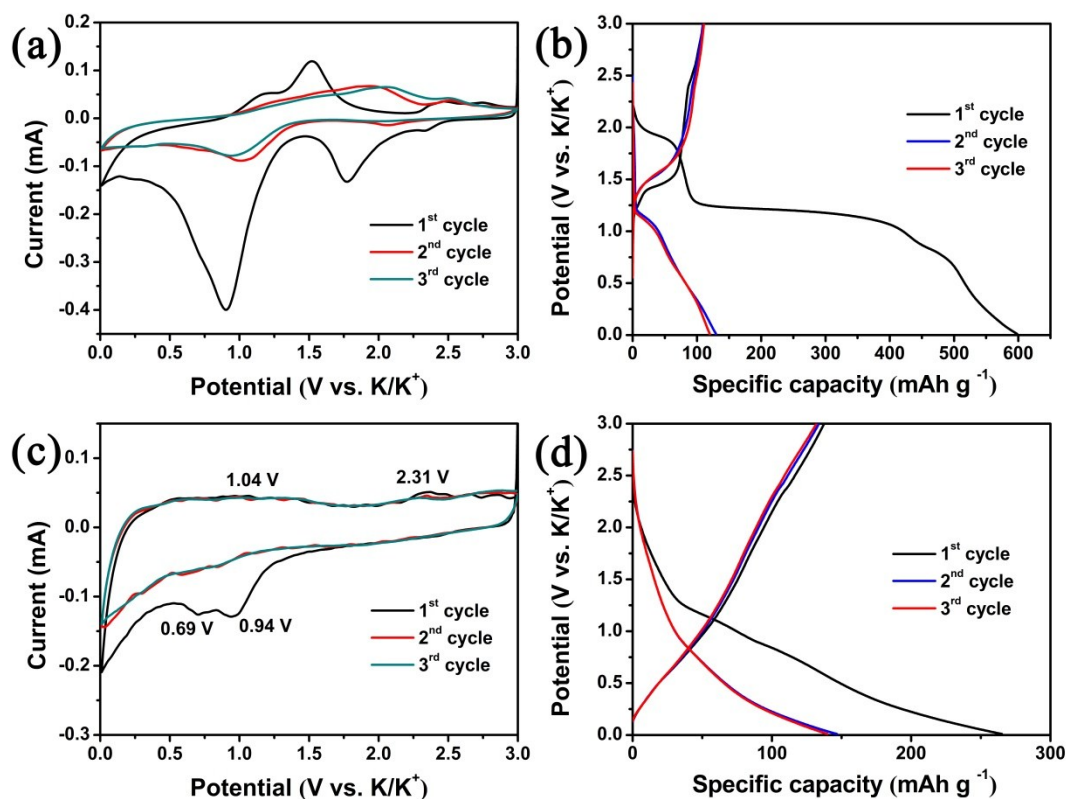


Fig. S8. The CV curves and Galvanostatic charge/discharge profiles of VS₄ (a, b), bare V₃S₄ (c, d), respectively.

The CV curve of VS₄ quite disagree with that of V₃S₄@NCNFs, which have strong cathodic/anodic peaks, in matching with the charge-discharge plateaus of VS₄, which demonstrate its obvious diffusion behavior not pseudocapacitive behavior. Regrettably, there is a large area loss for the CV curves from the first to the second cycle, demonstrating the poor reversibility for VS₄ as the anode in PIBs. The CV image of bare V₃S₄ is similar to that of V₃S₄@NCNFs, which agrees with the charge-discharge weak plateaus of V₃S₄. However, in the subsequent cycle, the V₃S₄ electrode shows the higher potentials of oxidation peaks and lower potentials of corresponding reduced peaks, indicating the large polarization for the potassium extraction/insertion process.^{1,2}

Table S1. Electrochemical performance comparison of vanadium-based and layered transition metal chalcogenides anode materials for PIBs.

Materials	Cycling Performance			Rate performance		Reference
	Discharge Capacity (mAh g ⁻¹)	Cycles	Current (mA g ⁻¹)	Discharge Capacity (mAh g ⁻¹)	Current (A g ⁻¹)	
V₃S₄@NCNFs	447 245	300 1000	200 2000	449, 410, 374, 346, 309, 249 and 202	0.1, 0.2, 0.5, 1.0, 2.0, 5.0 and 10	This work
VS₂ NSA	410 360	60 100	100 500	400, 380, 330, 250 and 100	0.1, 0.2, 0.5, 1.0 and 2.0	36
V₅S₈@C	501 190	100 1000	50 2000	550, 474, 422, 360, 312, 274, 205 and 153	0.05, 0.1, 0.2, 0.5, 1.0, 2.0, 5.0 and 10	37
VSe₂	335	200	200	374, 350, 334, 269 and 172	0.1, 0.2, 5, 1 and 2.0	53
VN-QDS	228 215	100 500	100 500	261, 215, 187 and 152	0.1, 0.5, 1 and 2.0	54
V₂O₃@PNCNFs	230	200	50	240, 221, 202, 186, 170 and 134	0.05, 0.1, 0.2, 0.3, 0.5 and 1	55
V₂O_{3-x}@rGO	162 104	500 2000	200 1000	250, 210, 175, 160, 127 and 104	0.025, 0.05, 0.1 0.2, 0.5 and 1.0	56
MoS₂/N-doped-C	212 151	200 1000	100 500	258, 238, 204, 171 and 131	0.1, 0.2, 0.5, 1 and 2	38
MoS₂@rGO	416.7 424.6	200 1000	100 500	438.5, 364.8, 302.9, 253 and 196.8	0.1, 0.2, 0.5, 1 and 2	29
WS₂	102.8	100	100	109, 99, 86, 74, 68 and 62	0.05, 0.1, 0.2, 0.4, 0.6 and 0.8	39

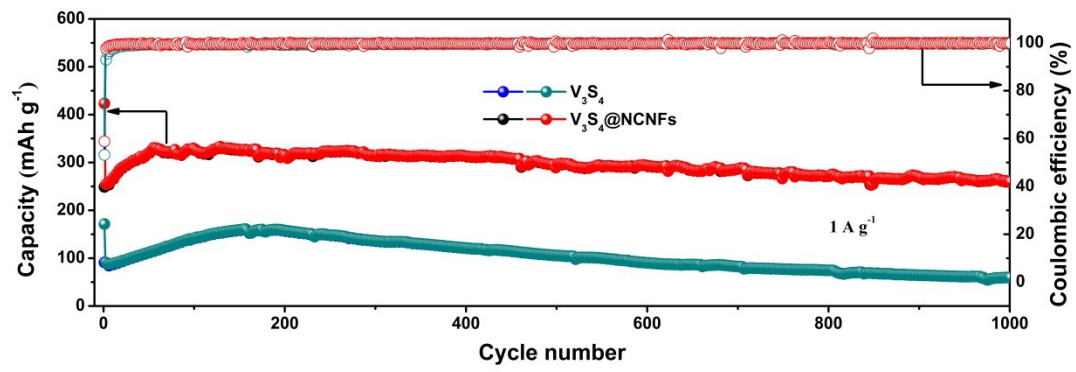


Fig. S9. Long-term cycling stability of the $V_3S_4@NCNFs$ and V_3S_4 electrodes at current densities of 1 A g^{-1} .

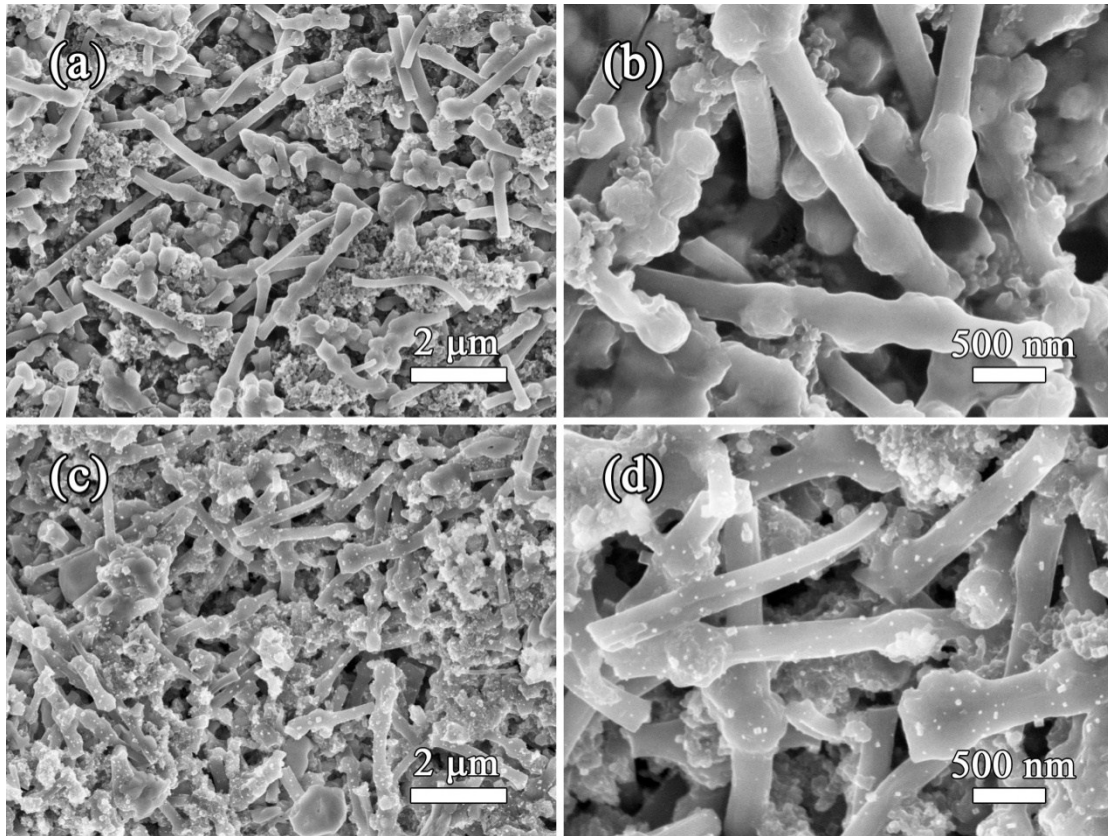


Fig. S10. Different magnifications SEM images of $V_3S_4@NCNFs$ electrode before cycling (a, b) and after 300 cycles at 0.2 A g^{-1} (c, d).

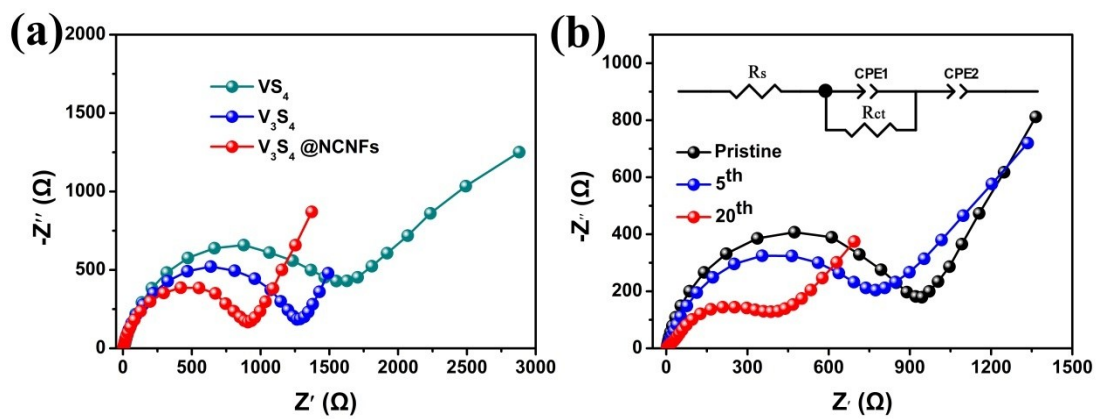


Fig. S11. (a) Nyquist plots of the VS_4 , bare V_3S_4 , and $V_3S_4@NCNFs$ electrodes. (b) Nyquist plots of the $V_3S_4@NCNFs$ electrodes after different cycles (inset: fitting equivalent circuit).

Table S2. The fitted results of hierarchical $V_3S_4@NCNFs$ based on the equivalent circuit model.

sample	R_s (Ω)	R_{ct} (Ω)
Before cycling	2.41	888
After 5 cycles	2.43	760
After 20 cycles	2.08	493

References

1. C. Mao, Y. Zhong, H. Shang, C. Li, Z. Guo and G. Li, *Chem. Eng. J.*, 2016, **304**, 511-517.
2. D. Zhang, Y. J. Mai, J. Y. Xiang, X. H. Xia, Y. Q. Qiao and J. P. Tu, *J. Power Sources.*, 2012, **217**, 229-235.